MEASUREMENT OF FATIGUE CRACK GROWTH RATES FOR STEELS IN HYDROGEN CONTAINMENT COMPONENTS

Somerday, B.P., Nibur, K.A. and San Marchi, C.
Sandia National Laboratories, 7011 East Ave., MS 9404, Livermore, CA, USA, 94550
corresponding author email: bpsomer@sandia.gov

ABSTRACT

The objective of this work was to enable the safe design of hydrogen pressure vessels by measuring the fatigue crack growth rates of ASME code-qualified steels in high-pressure hydrogen gas. While a design framework has recently been established for high-pressure hydrogen vessels, a material property database does not exist to support the design calculations. This study addresses such voids in the database by measuring the fatigue crack growth rates of three different heats of ASME SA-372 Grade J steel in 100 MPa hydrogen gas. Results showed that the fatigue crack growth rates were similar for all three steel heats, although the highest-strength steel appeared to exhibit the highest growth rates. Hydrogen accelerated the fatigue crack growth rates of the steels by as much as two orders of magnitude relative to anticipated crack growth rates in inert environments. Despite such dramatic effects of hydrogen on the fatigue crack growth rates, measurement of these properties enables reliable definition of the design life of steel hydrogen containment vessels.

1.0 INTRODUCTION

One of the safety issues related to containment of high-pressure hydrogen gas is the phenomenon of hydrogen embrittlement of structural materials. Hydrogen embrittlement is manifested in materials by reduced resistance to crack propagation, e.g., lower values of fracture toughness and accelerated rates of fatigue crack growth. As a result, the structural integrity of hydrogen containment components can be compromised. Although materials such as structural steels can exhibit quite pronounced effects of hydrogen embrittlement, such susceptibility to hydrogen embrittlement does not preclude the materials from consideration in hydrogen containment components. Rather, design methods that accommodate hydrogen embrittlement can be applied to quantify the service life of containment components.

A design method that accommodates hydrogen embrittlement was recently established for high-pressure hydrogen vessels. This design method was published as Article KD-10 (“Special Requirements for Vessels in High Pressure Gaseous Hydrogen Transport and Storage Service”) in Section VIII, Division 3 of the American Society of Mechanical Engineers (ASME) Boiler and Pressure Vessel Code [1]. The design approach in Article KD-10 is effective in addressing hydrogen embrittlement for the following reasons. First, the structural failure mode facilitated by hydrogen embrittlement is explicitly identified. In the case of pressure vessels subjected to pressure cycling, the governing failure mode is expected to be hydrogen-accelerated fatigue crack growth. Once the likely failure mode is identified, the appropriate analysis for quantifying the design life can be applied. The second key element in the design approach is specifying measurement of the relevant material properties. In this case, design life calculations require measurement of the fatigue crack growth rates of structural steels in the service environment, i.e., high-pressure hydrogen gas.

The objective of this work was to enable the safe design of hydrogen pressure vessels by measuring the fatigue crack growth rates of ASME code-qualified steels in high-pressure hydrogen gas. One class of steels currently used for hydrogen gas vessels is the ASME SA-372 series. These steels are candidates for higher-pressure hydrogen containment vessels with service pressures up to 100 MPa. While ASME Article KD-10 provides a design framework for these high-pressure vessels, a material property database does not exist to enable the design calculations. This study addresses such voids in the database by measuring the fatigue crack growth rates of an ASME SA-372 steel in 100 MPa hydrogen gas.

2.0 EXPERIMENTAL PROCEDURES

2.1 Description of Steels

Three different heats of steel were tested in this study, where the alloy composition, heat treatment, and mechanical properties of the steels conformed to the ASME SA-372 standard, "Specification for Carbon and Alloy Steel Forgings for Thin-Walled Pressure Vessels". The steels were manufactured to meet the alloy composition requirements for Grade J, which are listed in Table 1. The SA-372 steels are typically formed into seamless pipe, and qualification of the steel is performed on test rings removed from the seamless pipe. In this study, the SA-372 Grade J test rings were heat treated to qualify the steel as Class 70. The 61 cm-long test rings were heat treated using a one-sided quench followed by tempering. The tempering temperatures and mechanical properties measured for the three steels are summarized in Table 2. The mechanical property requirements for Class 70 steels are also included in Table 2, which indicates that the three steels qualified as Class 70.

Table 1. Concentration range for alloy elements in ASME SA-372 Grade J steel.

Cr (wt%)	Mo (wt%)	Mn (wt%)	Si (wt%)	C (wt%)	S (wt%)	P (wt%)	Fe (wt%)
0.80-1.15	0.15-0.25	0.75-1.05	0.15-0.35	0.35-0.50	<0.025	<0.025	Bal.

Table 2. Mechanical properties for Class 70 designation and for steels tested in this study.

Steel	Tempering Temperature (^{o}C)	Tensile Strength (MPa)	Yield Strength (MPa)	Elongation (%)
Class 70	>595	825-1000	>485	>18
Heat 1	660	839	642	22.0
Heat 2	657	871	731	19.3
Heat 3	657	908	784	24.0

2.2 Fatigue Crack Growth Measurements

Fatigue crack growth rate testing on the SA-372 Grade J steels was conducted following procedures in ASTM Standard E647-05. The test specimens were extracted from the steel test rings and designed according to the compact tension (CT) geometry. These specimens had the following dimensions: thickness = 6.3 mm; width = 26 mm; and precrack-starter notch length = 5.2 mm. The precrack-starter notch of the CT specimens was oriented parallel to the longitudinal axis of the seamless pipe.

The CT specimens were prepared for testing by first cleaning the as-machined specimens in isopropyl alcohol. Following procedures in ASTM Standard E647-05, a precrack was propagated from the starter notch in each specimen by applying cyclic loading. This precracking process was conducted in air under the following mechanical conditions: load cycle frequency = 15 Hz; ratio of minimum load to maximum load (R) = 0.1; and final maximum stress-intensity factor (K_{max}) = 10 MPa·m$^{1/2}$. The precrack was propagated a distance of 1.8 mm from the notch tip to create a total precrack length-to-width ratio of 0.265.

Fatigue crack growth tests were conducted on the SA-372 Grade J compact tension specimens in hydrogen gas using a customized laboratory apparatus consisting of a pressure vessel inserted into the load train of a servo-hydraulic mechanical test frame. Each precracked CT specimen was placed in the pressure vessel and coupled to a pull rod penetrating through the bottom cover of the vessel. After the pressure vessel was sealed, residual air was purged from the gas manifold and pressure vessel using a

sequence of backfilling and venting through a check valve. Three backfilling/venting cycles were conducted with 21 MPa helium gas followed by three more with 21 MPa hydrogen gas. The pressure vessel was then filled with hydrogen gas (99.9999% purity) to the test pressure of 100 MPa. Each CT specimen was exposed to hydrogen gas in the vessel for approximately 15 to 20 h prior to mechanical loading. No net load was applied to the CT specimen by the pull rod when the vessel was pressurized, since a secondary chamber was designed into the vessel to ensure the pull rod was pressure balanced.

The fatigue crack growth tests in hydrogen gas were executed following guidance in ASTM Standard E647-05. The CT specimens were subjected to cyclic loading between fixed minimum and maximum loads, where the ratio of minimum load to maximum load, R, was equal to 0.5. This loading format lead to increasing values of stress-intensity factor range (ΔK) as the crack extended. The loading and unloading rates were programmed to be constant in each cycle (i.e., triangular loading wave form) using a load cell external to the pressure vessel as the feedback transducer in the control loop. As a result of friction forces on the pull rod from polymer sliding seals, the loading rate on the CT specimen in the pressure vessel varied during the loading and unloading segments. The load sustained by the CT specimen was measured using a load cell internal to the pressure vessel. Flexure of this customized load cell was measured with a linear variable differential transformer (LVDT), which was less sensitive to hydrogen gas than conventional strain gauges. Crack extension in the CT specimen was continuously monitored and quantified using the direct current potential difference (DCPD) technique, where the applied current was about 2 A. Data were digitally recorded at two points in each load cycle corresponding to the minimum and maximum loads. The recorded data included loads from both the external and internal load cells, the front-face crack opening displacement (measured using an LVDT), and the DCPD voltage.

One of the testing variables that received particular attention was the load cycle frequency, which was selected at 1 Hz to balance efficiency and effectiveness in the testing. Fatigue crack growth testing can be conducted more efficiently, i.e., test duration decreases, as frequency increases. However, since fatigue crack growth rates of steels in hydrogen gas are known to decrease as load cycle frequency increases, the test frequency must be limited so that measured crack growth rates are not unrealistically low. A frequency of 1 Hz allowed each test to be conducted efficiently, since the test duration was less than 3 h. Furthermore, although fatigue crack growth rates of steels in hydrogen are quite sensitive to frequency at values above 1 Hz, crack growth rates change more mildly as a function of frequency below 1 Hz [2] suggesting that 1 Hz may be an effective test frequency.

Termination of the fatigue crack growth tests was based on a maximum stress-intensity factor, i.e., K_{max} = 50 MPa·m$^{1/2}$. At this point, the crack length-to-width ratio was approximately 0.56. The data analysis consisted principally of calculating the crack length in each load cycle using the DCPD data recorded at maximum load. The crack length *vs* load cycle data were condensed into a set of average crack length data, where an average crack length was calculated for each successive set of 50 points. For these data intervals, average values of minimum and maximum loads were also calculated. The crack growth rate data (i.e., crack growth increment per cycle, da/dN) were determined by applying the secant method in ASTM E647-05 to the average crack length data. In this case, the crack growth increment (Δa) between successive average crack lengths was divided by the number of load cycles in the respective data averaging intervals, e.g., 50. The stress-intensity factor range, ΔK, associated with each da/dN data point was calculated at the mid-point between successive average crack lengths.

3.0 RESULTS AND DISCUSSION

Fatigue crack growth rate data are typically plotted as the crack growth increment per cycle, da/dN, *vs* the stress-intensity factor range, ΔK, on logarithmic coordinate axes. Such da/dN *vs* ΔK plots for the three heats of SA-372 Grade J steels tested in 100 MPa hydrogen gas are shown in Fig. 1. The plots exhibit the expected positive slope and a linear relationship between log(da/dN) and log(ΔK) over some range of ΔK.

The data in Fig. 1(a) demonstrate that fatigue crack growth rates for the SA-372 Grade J steels are similar over the range of ΔK examined in this study. The *da/dN* data show particular convergence at lower ΔK, but this effect is exaggerated by the pronounced noise in the data. The data noise is likely due to the relatively modest change in crack growth rates at lower ΔK coupled with the method used to calculate *da/dN*, i.e., the secant method. At higher crack growth rates, the noise diminishes and the data trends become more apparent. Two trends are particularly notable: the crack growth rates tend to be more rapid for the highest-strength steel (Heat 3) and there is a distinct change in slope of the *da/dN vs* ΔK relationships for all three steels at a ΔK value between 15 and 20 MPa·m$^{1/2}$. The slope changes are difficult to discern in Fig. 1(a), so one of the data sets (Heat 3) is plotted separately in Fig. 1(b) to more clearly illustrate this feature.

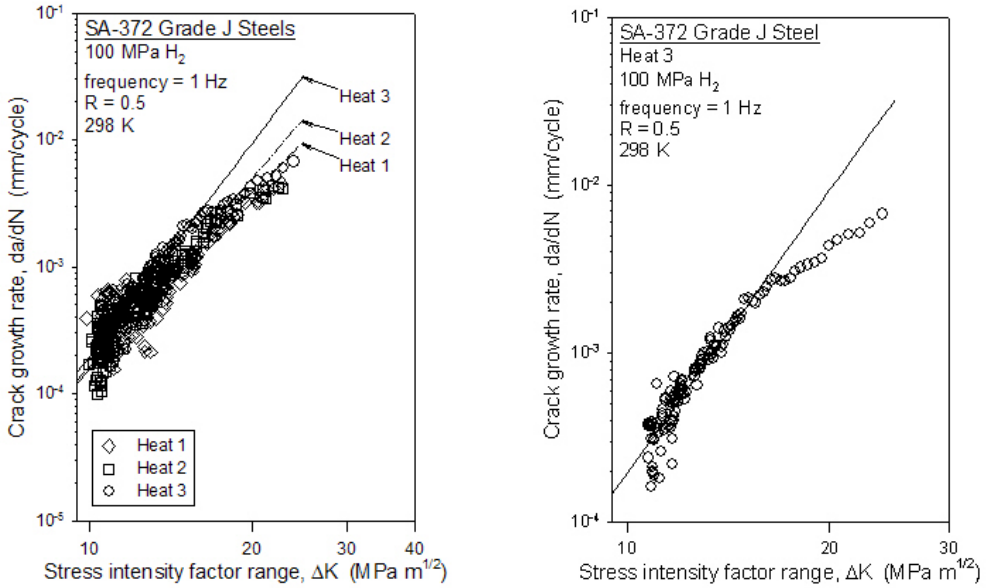

(a) **(b)**

Figure 1. (a) Fatigue crack growth rate plots for the three SA-372 Grade J steels in 100 MPa H_2 gas. (b) Fatigue crack growth rate plot for Heat 3 of SA-372 Grade J steel in 100 MPa H_2 gas.

Fatigue crack growth rate plots typically exhibit a linear relationship between log(*da/dN*) and log(ΔK) over some range of ΔK, i.e.:

$$\frac{da}{dN} = C\Delta K^m \tag{1}$$

where *C* and *m* are constants that depend on the material and the test environment. This relationship fits the data for each steel in Fig. 1 over the lower range of ΔK, i.e., prior to the slope change at ΔK values between 15 and 20 MPa·m$^{1/2}$. Establishing the *da/dN vs* ΔK relationship for the lower range of ΔK is most relevant for design life calculations, since the largest fraction of structural life is associated with lower ΔK values. The *C* and *m* values calculated from curve fits to the lower-ΔK data are provided in Table 3. The lines in Fig. 1 were constructed using Equation 1 and the parameters in Table 3.

Fatigue crack growth rates of steels in hydrogen gas exceeding 10 MPa pressure have not been measured extensively. One of the few sets of fatigue crack growth rate data identified for low-alloy

steels in high-pressure hydrogen gas is shown in Fig. 2. Here, fatigue crack growth rate data for the Ni-Cr-Mo steel HY-100 in 52 MPa hydrogen gas and 52 MPa helium gas [3] are compared to the crack growth rate data for the three SA-372 Grade J steels in 100 MPa hydrogen gas. The crack growth rates for the SA-372 Grade J steels can be about an order of magnitude greater than those for the HY-100 steel, and this difference is attributed to the effect of hydrogen gas pressure and not differences in material characteristics between the two steels. Evidence demonstrates that fatigue crack growth rates of steels can significantly increase as hydrogen gas pressure increases [2]. The data in Fig. 2 also illustrate the dramatic effect of hydrogen embrittlement in accelerating fatigue crack growth rates. Assuming that the two low-alloy martensitic steels SA-372 Grade J and HY-100 have similar fatigue crack growth rates in helium gas, the data in Fig. 2 show that fatigue crack growth rates in 100 MPa hydrogen gas can be two orders of magnitude greater than crack growth rates in helium gas.

Table 3. Parameters in fatigue crack growth relationships for SA-372 Grade J steels in 100 MPa H_2.

Steel	C (mm/cycle)	m
Heat 1	4.2×10^{-9}	4.6
Heat 2	1.9×10^{-9}	4.9
Heat 3	5.1×10^{-10}	5.6

Comparison of *da/dN vs ΔK* data can demonstrate the relative sensitivity of materials to hydrogen embrittlement, however such comparisons do not enable quantitative design evaluations of hydrogen containment structures. The *da/dN vs ΔK* relationship must be used in conjunction with structural analysis to establish the design life of a hydrogen containment component. This fatigue crack growth-based component design approach is employed in ASME Article KD-10 for hydrogen containment vessels. The basic objective of the design approach is depicted schematically in Fig. 3.

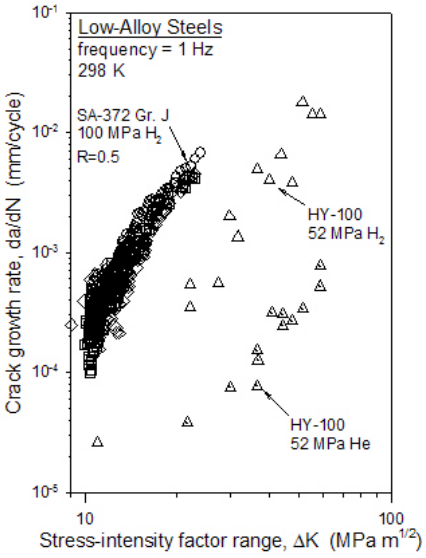

Figure 2. Fatigue crack growth rate plots for the three SA-372 Grade J steels in 100 MPa H_2 gas compared to plots for the Ni-Cr-Mo steel HY-100 in 52 MPa H_2 gas and 52 MPa He gas [3].

The design concept in Fig. 3 is based on the assumption that a hydrogen containment component (e.g., a pressure vessel) contains an existing flaw on the interior surface (with a depth dimension, a_o), and

this flaw propagates principally under the action of pressure cycles (i.e., wall stress cycles). The intent of the design approach is to calculate the crack depth (a) as a function of the number of pressure cycles (N). The basic element of the design calculation is the fatigue crack growth law (e.g., Equation 1). Based on the applied pressure range and component dimensions, the stress-intensity factor range, ΔK, can be calculated at the instantaneous crack depth. This ΔK value is input into the fatigue crack growth law to calculate an increment of crack growth for the pressure cycle. The crack depth is then updated, and a new ΔK value and increment of crack growth can be calculated. This series of calculations leads to the construction of the crack depth *vs* number of cycles curve in Fig. 3. The curve is truncated at a critical crack depth (a_c) associated with the onset of a new failure mode characterized by rapid crack extension.

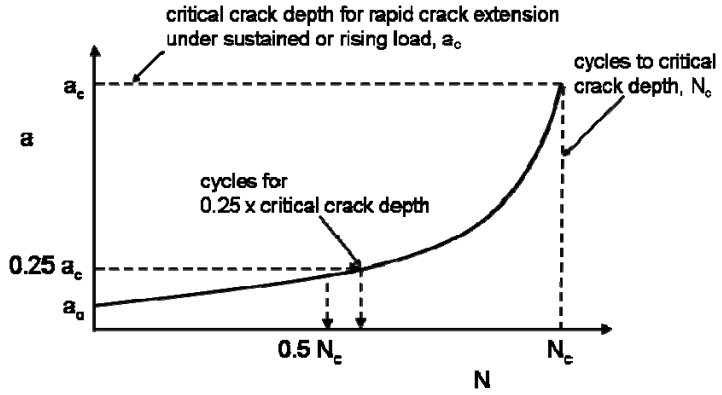

Figure 3. Schematic of the crack depth (a) *vs* number of pressure cycles (N) construction for a pressure vessel designed based on a fatigue crack growth failure mode.

The fatigue crack growth-based design method reflected in Fig. 3 is an effective approach for assuring the safety of hydrogen containment structures that are susceptible to hydrogen embrittlement and subjected to pressure cycling. Once the crack depth *vs* number of pressure cycles curve is constructed, a limiting number of pressure cycles can be imposed on the structure. For example, the ASME Article KD-10 identifies the limiting number of pressure cycles as the lower value of either 50% of the number of cycles at the critical crack depth (N_c) or the number of cycles to reach 25% of the critical crack depth (see Fig. 3). The rationale for choosing these limits is to preclude the crack from extending to the point where its growth rate starts to increase rapidly, i.e., the point where the slope of the *a vs N* curve starts to increase rapidly. Having a reliable method to calculate the crack depth as a function of service history coupled with periodic inspection allows safety margins to be established for hydrogen containment components.

4.0 CONCLUSIONS

- The fatigue crack growth relationships (*da/dN vs* ΔK) were measured for three different heats of ASME SA-372 Grade J steel in 100 MPa hydrogen gas. The fatigue crack growth rates were similar for all three steel heats, although the highest-strength steel appeared to exhibit the highest growth rates.

- Hydrogen accelerated the fatigue crack growth rates of the SA-372 Grade J steels by as much as two orders of magnitude relative to anticipated crack growth rates in inert environments.

- The *da/dN vs* ΔK relationships measured in hydrogen gas serve as the foundation for fatigue crack growth-based design calculations that demonstrate the safe operation of hydrogen containment components.

ACKNOWLEDGMENTS

The authors acknowledge J. Felbaum for supplying the test specimens and K. Lee for assistance in conducting the fatigue crack growth tests in high-pressure hydrogen gas. Sandia is a multi-program laboratory operated by Sandia Corporation, a Lockheed Martin Company, for the United States Department of Energy under contract DE-AC04-94AL85000.

REFERENCES

1. Rana, M.D., Rawls, G.B., Sims, J.R. and Upitis, E., Technical Basis and Application of New Rules on Fracture Control of High Pressure Hydrogen Vessel in ASME Section VIII, Division 3 Code, Proceedings of 2007 ASME Pressure Vessels and Piping Division Conference, 22-26 July 2007, San Antonio, TX, Paper No. PVP2007-26023.
2. Priest, A.H., Fatigue Crack Growth and Fracture Resistance of Steels in High-Pressure Hydrogen Environments, Commission of the European Communities, Luxembourg, Contract No. EHC-(1)42-012-81UK(H), 1983.
3. Walter, R.J. and Chandler, W.T., Influence of Gaseous Hydrogen on Metals Final Report, NASA, Marshall Space Flight Center, AL, Report No. NASA-CR-124410, 1973.